Stability Improvement of High-Pressure-Ratio Turbocharger Centrifugal Compressor by Asymmetrical Flow Control—Part II: Nonaxisymmetrical Self-Recirculation Casing Treatment

Xinqian Zheng
e-mail: zhengxq@tsinghua.edu.cn

Yangjun Zhang

Mingyang Yang

State Key Laboratory of Automotive Safety and Energy,
Tsinghua University,
Beijing 100084, China

Takahiro Bamba

Hideaki Tamaki

Turbo Machinery and Engine Technology, Department, IHI Corporation,
Yokohama, 235-8501, Japan

This is part II of a two-part paper involving the development of an asymmetrical flow control method to widen the operating range of a turbocharger centrifugal compressor with high-pressure ratio. A nonaxisymmetrical self-recirculation casing treatment (SRCT) as an instance of asymmetrical flow control method is presented. Experimental and numerical methods were used to investigate the impact of nonaxisymmetrical SRCT on the surge point of the centrifugal compressor. First, the influence of the geometry of a symmetric SRCT on the compressor performance was studied by means of numerical simulation. The key parameter of the SRCT was found to be the distance from the main blade leading edge to the rear groove (S_r). Next, several arrangements of a nonaxisymmetrical SRCT were designed, based on flow analysis presented in part I. Then, a series of experiments were carried out to analyze the influence of nonaxisymmetrical SRCT on the compressor performance. Results show that the nonaxisymmetrical SRCT has a certain influence on the performance and has a larger potential for stability improvement than the traditional symmetric SRCT. For the investigated SRCT, the surge flow rate of the compressor with the nonaxisymmetrical SRCTs is about 10% lower than that of the compressor with symmetric SRCT. The largest surge margin (smallest surge flow rate) can be obtained when the phase of the largest S_r is coincident with the phase of the minimum static pressure in the vicinity of the leading edge of the splitter blades. [DOI: 10.1115/1.4006637]

1 Introduction

High-pressure-ratio turbocharging plays an important role in vehicle engines nowadays for its prominent advantage in emission control and power density improvement [1,2]. The need for significantly downsizing the engine to reduce fuel consumption as well as for the high rate of exhaust gas recirculation to reduce NO_x emission calls for a high-pressure-ratio turbocharger with a wide operating range to meet the requirement of engines [3]. Finally, a high altitude operation makes a high-pressure-ratio turbocharger indispensable to recover the engine power [4]. The centrifugal compressor is the critical component in a high-pressure-ratio turbocharger, as it determines the flow range of the device. High-pressure-ratio compressors in general need higher circumferential velocities than conventional designs with lower pressure ratio which results in increased Mach number and very often in transonic flow conditions in the machine. It is well known that compressors with transonic flow often suffer from low efficiencies and reduced flow margin. This is believed to be due to the impact of shocks and shock/boundary layer interactions [5]. The latter flow phenomenon causes flow separation, strong vortex flow, or vortex breakup, which will force the compressor to stall [6].

A lot of research has been done to improve the flow range of high-pressure-ratio centrifugal compressors [7–10]. Generally there are two types of stability enhancement. One is an active control method, which has been comprehensively investigated in axial and centrifugal compressors. Extra instruments such as speakers are required for this kind of treatment. This is not suitable for mass-manufactured turbochargers. Another one is passive control method, which makes some adjustment on the compressor geometry only and is more feasible for vehicle turbochargers.

Self-recirculation casing treatment (SRCT) is a widely used passive control method to extend the operating range of high-pressure-ratio centrifugal compressors. Experimental research on SRCT was first performed on a vehicle turbocharger centrifugal compressor by Fisher [11]. It was concluded that the pressure gradient between the slots drove the flow recirculation through the casing. When the compressor was operated near stall condition, the low-momentum flow near the shroud of the impeller was sucked into the casing and forced to move toward the main flow upstream due to the inverse pressure gradient. As a result, the incidence of the impeller was reduced and the stability was enhanced. The influence of the casing treatment geometry on the centrifugal compressor performance was investigated by numerical simulation [12–15]. It was found that the layout as well as the geometrical parameters of the rear groove

Contributed by the International Gas Turbine Institute (IGTI) of ASME for publication in the JOURNAL OF TURBOMACHINERY. Manuscript received April 26, 2010; final manuscript received December 26, 2011; published online November 1, 2012. Assoc. Editor: Michael Casey.

have a significant impact on compressor performance. Therefore, the optimization of the treatment geometries should be focused on layout and rear groove.

However, the traditional SRCT on the centrifugal compressor is unexceptionally symmetric in the circumferential direction. The asymmetrical flow phenomenon in centrifugal compressors is not considered in the development of this kind of flow control method. In light of the findings from part I of this paper, it can be stated that static pressure asymmetries in the circumferential direction appears throughout the entire compressor. Since the inverse static pressure gradient in the impeller is responsible for the recirculation flow in the casing, the recirculation flow rate in the circumferential direction is inevitably different from position to position and the effect of compressor stability enhancement must be affected by the asymmetry.

It has been confirmed for axial compressors that the nonaxisymmetrical casing treatment has a positive effect on stability [16–18]. However, the consideration of this kind of casing treatment was the nonaxisymmetrical tip clearance because of assembly or operating instead of intrinsical asymmetry. It was documented in part I that an intrinsical asymmetrical flow field can be found in a centrifugal compressor. Hence, it is reasonable to develop a kind of asymmetrical flow control method to exploit benefits that can be extracted from the intrinsic asymmetries.

Based on the conclusions of part I, the effectiveness and mechanism of nonaxisymmetrical SRCT on flow control was investigated in part II. Experimental testing and numerical simulation were employed for this paper.

2 Numerical Methods

Numerical simulation was employed to investigate the influence of the geometry on performance as well as the detailed flow field in the compressor. The solver applies a CFD code based on a three-dimensional (3D) steady compressible finite volume scheme to solve the Reynolds-averaged Navier-Stokes equations. A central scheme was used for spatial discretization while a fourth-order Runge-Kutta scheme was used for temporal discretization. For the turbulence model, the Spalart-Allmaras 1-equation model was adopted. Total temperature and pressure together with the velocity direction were imposed as inlet boundary conditions; static pressure was set as outlet boundary condition. No-slip and impermeability conditions were imposed on the impeller blade surface. More detailed information can be found in part I.

The grid quality in the meshed SRCT is of utmost importance for the flow simulation in this work. In general, great steps in cell size induces numerical problems for CFD solvers. As for cell size, SRCT and passage mesh usually differ significantly; hence matching these two grids is a challenging issue. Figure 1 illustrates the topology of a promising approach for the tip clearance grid, which was used in this work. The clearance mesh attached to the passage is divided into three levels. The first level grid matches with the blade tip; the second level grid covers the whole passage and has a smaller size than that of the passage and the first level; and the third level grid is divided into three blocks, of which the middle block matches with the SRCT grid in cell size. All the tip clearance grid blocks rotate except the middle block in the third level. The frozen rotor approach is employed to model the interfaces between rotor and stator blocks. The other interfaces are set as full nonmatching boundary conditions. One single passage was used as computational domain to identify the key parameters, while the whole stage including all the passages, the diffuser, and the volute was used to study the detailed flow. The computational domain is shown in Fig. 2. There were 890,000 nodes in total for a single passage and approximately 12,100,000 for the whole stage (with SRCT). The grid cells number of a single passage is much larger than that required by grid independence, as discussed in part I.

Because compressor stall or surge is a strongly unsteady process, the steady simulation is not suitable to predict the initiation point of the stall precisely. But it has often been employed to predict the compressor performance map because of the promising CPU time requirements. Generally, the point where the steady simulation begins to blow up is considered to be the stall point. The unsatisfying inlet boundary condition caused by the recirculation flow at the inlet was the main reason for the numerical stall. As a result, the predicted stall point should be closely related to the inlet grid domain, which makes the stall initiation prediction casual. However, it is reasonable to compare the stall points by

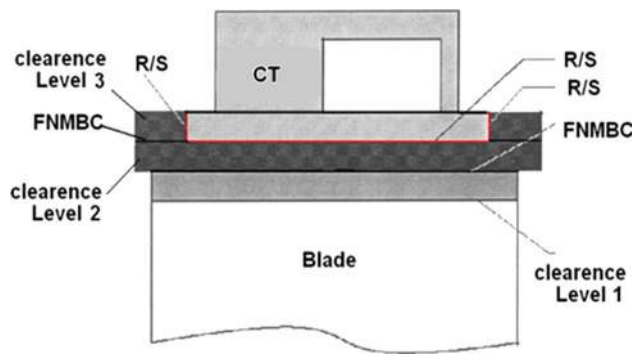

Fig. 1 Sketch of meshing approach for tip clearance

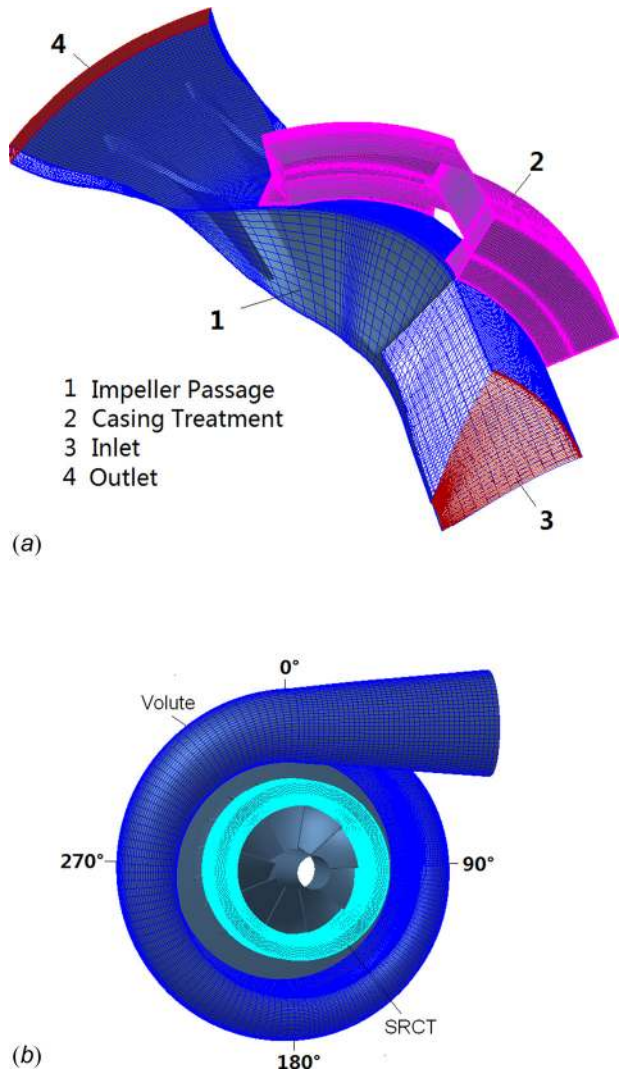

Fig. 2 The computational domain of single passage and whole stage

steady simulation among different kinds of compressor with the same inlet domain as well as the other boundaries. In the present analysis, the blowing up point was considered to be the stall point, as usual.

3 The Influence of the SRCT Geometry

In order to reduce the driving power, the investigated centrifugal compressor is precisely half scaled from the one in part I. The flow phenomenon can be considered to be similar in the two compressors. Therefore, the impeller diameter of the investigated compressor is 75 mm and the designed rotational speed N is 130,000 rev/min. The sketch of the SRCT in a centrifugal compressor is shown in Fig. 3. Six parameters were used to describe the SRCT geometry. In order to develop the nonaxisymmetrical SRCT suitable to the nonaxisymmetrical flow in a centrifugal compressor, numerical simulation was used to determine the key geometric parameters which have the greatest impact on the compressor performance. Each parameter was investigated with all other parameters kept constant, including topology and grid number. The matrix of the baseline SRCT geometry parameters is given in Table 1. The geometric parameters in axial direction are scaled by the distance between the main blade leading edge and splitter leading edge, and the parameters in radial direction are scaled by the inlet tip radius.

Figures 4 and 5 show the performance comparison of the centrifugal compressor with different SRCT types at the design flow rate. The geometrical parameters are normalized by the corresponding baseline parameters in Table 1.

It can be seen from Figs. 4 and 5 that the geometry of the rear groove S_r, the width of the rear slot b_r, have the most evident influence on centrifugal compressor pressure ratio as well as the efficiency. As the parameters increase, the pressure ratio generally decreases while the efficiency first decreases then goes up. The reason for the influence on compressor performance by the SRCT is the recirculation flow. The parameter which has the most influence on the recirculation flow has the most evident influence on the compressor performance. Taking the parameter S_r for example, as S_r increases, the rear groove is moved away from the main blade leading edge. Therefore, the pressure gradient in the SRCT increases then the recirculation flow increases. Figure 6 shows the influence on recirculation flow rate by geometric parameters. The flow rate is dimensionless by the impeller inlet flow rate. It could be noticed that again the two parameters (S_r, b_r) have the most evident influence on the recirculation flow. As S_r and b_r increases, the increasing recirculation flow in the SRCT contributes to more flow loss in the SRCT due to the higher flow velocity and larger flow rate. As a result, the pressure ratio of the compressor generally decreases.

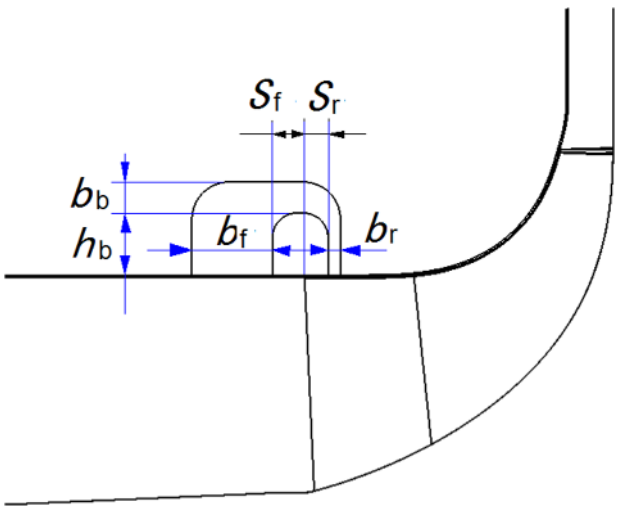

Fig. 3 Sketch of SRCT in a centrifugal compressor

Table 1 SRCT parameters

S_r	S_f	b_r	b_f	b_b	h_b
0.148	0.278	0.089	0.185	0.236	0.145

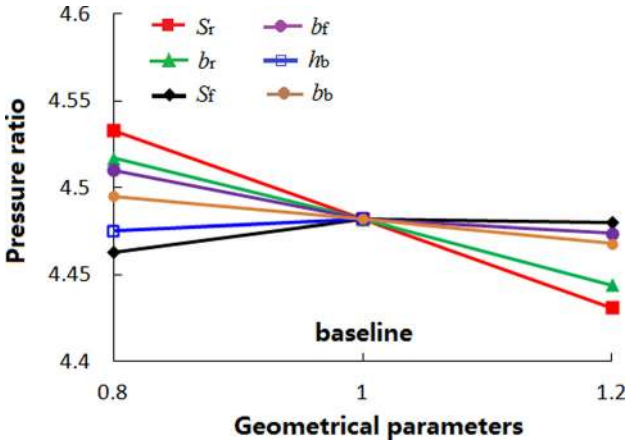

Fig. 4 Influence of SRCT geometry on the compressor pressure ratio

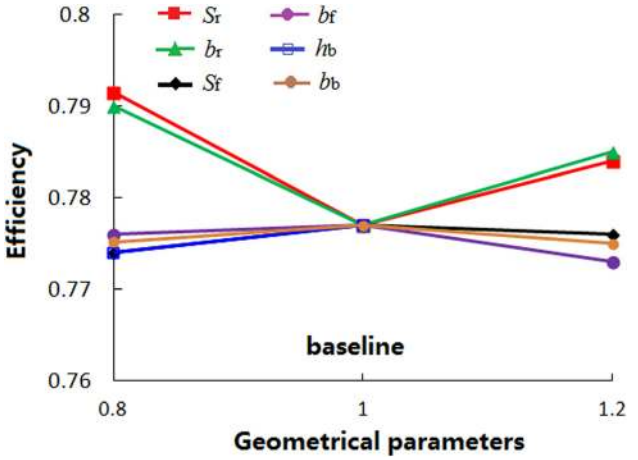

Fig. 5 Influence of SRCT geometry on the efficiency

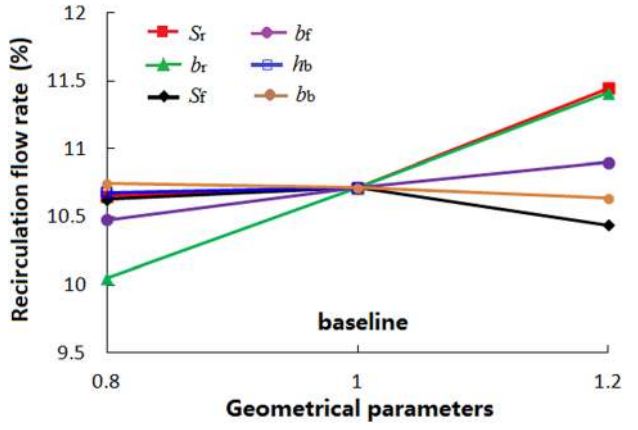

Fig. 6 Influence of SRCT geometry on the recirculation flow rate

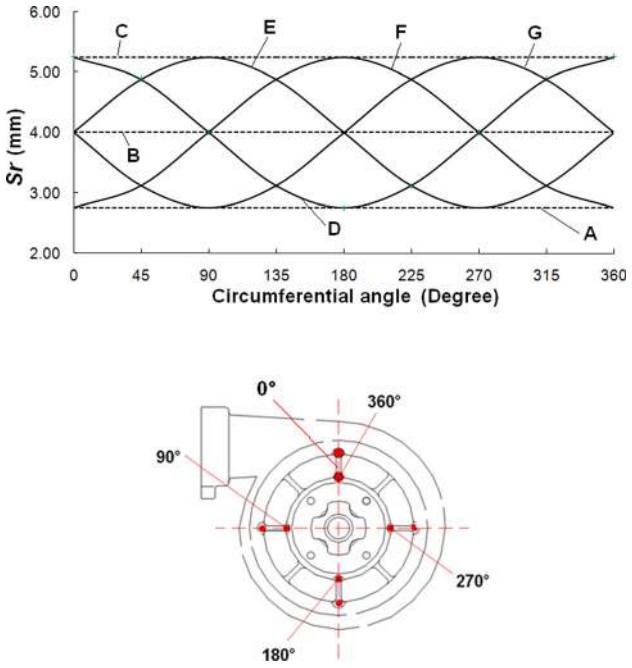

Fig. 7 Circumferential S_r distribution for seven SRCT types

With regards to the information in Figs. 4–6, it can be concluded that the distance between the rear groove of the SRCT and the main blade leading edge (S_r) was one of the key geometric parameters. Although the geometries influence at other speeds has not been investigated, it is reasonable to hold the similar conclusion. This is taken as the basis for the development of the nonaxisymmetrical SRCT. That means, only S_r is different in the circumferential direction in order to develop nonaxisymmetrical SRCT in this paper.

4 Experimental Facilities

In order to investigate the effectiveness of nonaxisymmetrical SRCT, S_r is designed with a sinusoidal distribution in the circumferential direction and the other geometric parameters of the SRCT are symmetric, which are given in Table 1. Four arrangements of this nonaxisymmetrical SRCT with different initial phases were investigated, named D, E, F, and G as shown in Fig. 7. The maximum, average, and minimum of the S_r is 5.25, 4.00, and 2.75 mm, respectively. The maximum value of S_r for D, E, F, and G is located at 0 deg, 90 deg, 180 deg, and 270 deg, respectively. The vertical direction is defined as 0 deg as the referential position, as shown in Fig. 7. In order to compare with nonaxisymmetrical SRCT, three kinds of symmetric SRCT A, B, and C are designed with values of 2.75, 4, and 5.25 mm for S_r, respectively.

Usually, the shroud of the impeller is integrated in the volute for a turbocharger compressor. However, it is not easy to mill the nonaxisymmetrical SRCT in this kind of volute. Therefore, the shroud of impeller and vaneless diffuser are separated from the volute. The nonaxisymmetrical groove was milled on the shroud, as shown in Fig. 8. Different types of nonaxisymmetrical SRCT can thus be obtained by rotating the relative position between shroud and volute.

A turbocharger experimental rig was used to obtain the centrifugal compressor performance. Pressurized air, which was supplied by a larger displacement compressor, was heated in a combustion chamber in front of the turbine, and then expanded in the turbine to drive the compressor to rotate at a certain speed. The speed of the turbocharger was controlled by the valve in front of the turbine, by which the flow rate in the turbine was controlled. The flow rate in the compressor was controlled by a valve at the outlet of the compressor. All measured parameters were gathered and analyzed automatically in the control platform.

The major parameters measured during the performance testing included total/static pressure and temperature at the inlet/outlet of the compressor, flow rate, rotational speed, as well as ambient pressure and temperature. The temperature was measured by thermocouples with an error of less than ± 1 °C; Pressure was measured by DSA3017 pressure sensor with an error of less than $\pm 0.2\%$; flow rate was measured by the vortex flow meter with an error of less than $\pm 1.0\%$; rotational speed was measured by an electromagnetic transducer with an error less than 0.5%.

The reliable determination of surge points in experimental testing is always difficult but important for a complete centrifugal compressor map. Several methods were used to determine the surge points. For example, a dynamic probe or a hot wire was employed to capture the surge initiation and derive the information about compressor surge [19–21]. The results showed that periodic oscillation with evident amplitude was the sign of surge. They are reliable methods for surge determination supposing that oscillation signal is well captured and identified. Another method of surge determination, which was applied in this paper, is via specific acoustic phenomena in the surge process assisted by the compressor performance in real time. The "sewing machine whistle" is a distinct cyclic noise caused by unstable compressor operating conditions known as compressor surge. Just at the beginning of the sewing machine whistle occurring, the surge point is determined in the performance map. It seems that the former method to find the surge point is more credible because the oscillation could be immediately identified by instruments as the surge is encountered. On the hand, the latter method has reasonable reliability and is widely applied due to its convenience.

5 Results and Analysis

5.1 Experimental Results

5.1.1 Results With Symmetric SRCT. Figure 9 shows the comparison of the surge rates of compressors with three different symmetric treatments A, B, C, and the original case without an SRCT. The x axis in Fig. 9 is rotational speed, which is normalized by the designed speed N (as well as in the following figures). The

Fig. 8 Separated shroud with SRCT and volute

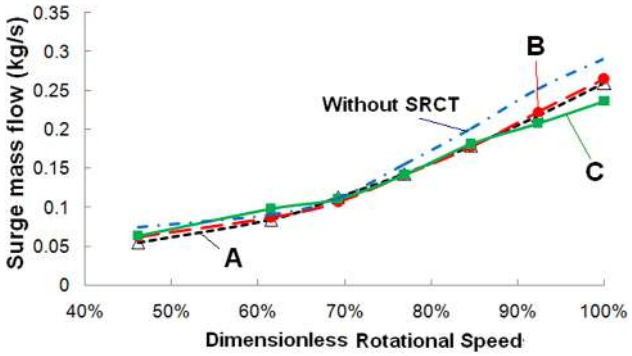

Fig. 9 Comparison of surge flow rates for compressors with symmetric SRCTs

purpose of this paper is to develop asymmetrical flow control method to widen the flow range. Therefore, the efficiency and the pressure ratio of the compressor with and without SRCT is not present in this paper. It can be seen from Fig. 9 that the surge line curves intersect complicatedly with each other at different speeds, which means that one type of SRCT is not able to optimize while improving *Ms* at all speeds. It can be seen that for speed lower than 70%*N*, the compressor with type A SRCT and with the smallest S_r has the smallest surge flow rate. The compressor with type C SRCT, with the largest S_r, has the largest surge flow rate. However, as the speed increases to 90%*N* or above, type C SRCT has the smallest surge flow rate. This advantage becomes more evident as speed increases. When a compressor is operated at higher speed, the pressure ratio is usually higher. Once the compressor approaches surge condition, the one with the larger S_r will have a larger recirculation flow rate than the one with smaller S_r or when it is operated at lower speeds. The surge flow rate therefore decreased. However, when the compressor is operated at lower speeds, the surge flow rate is smaller for the compressor with small S_r. Investigation indicated the compressor performance with larger S_r will deteriorate at low speed for small flow rate due to excessive inlet recirculation flow rate [21]. A similar situation existed in the experiment results which compared the maps between compressors with and without SRCT, in which the surge flow rate was larger for the one with SRCT at low speeds [15]. So, the rear groove position S_r is very important. If the surge margin is too small at a lower pressure ratio (lower speed), the S_r should be designed smaller; if the surge margin is too small at higher pressure ratio (higher speed), the S_r should be designed larger.

5.1.2 Results With Nonaxisymmetrical SRCT. Figure 10 shows the comparison of surge flow rates for the four cases with nonaxisymmetrical SRCT, D–G. The nonaxisymmetry is given to SRCT by circumferentially varying the rear groove position according to sinusoidal functions. The shape of S_r for the four cases was completely identical, only the phase of the sinusoidal distribution was different. However, significant different results were obtained. That means, the groove nonaxisymmetry has certain influence on performance. If the flow field of the impeller is symmetric, the results for the four cases with nonaxisymmetrical SRCT should be fully identical. So, the asymmetrical characteristic of the flow field is the basis for developing the asymmetrical flow control method.

Figure 10 also shows that the difference in surge flow rate becomes more significant as the rotational speed increases. The reasons for that are as follows. First, the asymmetry is larger as the rotational speed increases, which is confirmed in part I. Second, because the stall incidence at the inducer is smaller as the Mach number is larger, the stability at higher speed with higher Mach number is expected to exhibit a significantly higher sensitivity to an asymmetrical characteristic of the flow field.

5.1.3 Mechanism Analysis of Nonaxisymmetrical SRCT. As it was discussed before, the static pressure in the impeller is the force driving the recirculation in the casing treatment. The varying effect on the surge flow rate for different SRCTs should be related to the static pressure distribution in the impeller. Figure 11 shows the static pressure distribution near the tip of the leading edge of the splitter blades, which was carefully analyzed in part I. There is an evident static pressure distortion in the circumferential direction. Magnitude and phase vary with rotational speeds.

In order to make comparison convenient, a nondimensional surge margin *Ms* was defined in following equation:

$$Ms = \frac{M_{\text{org}} - M}{M_{\text{org}}} \tag{1}$$

Figure 12 shows *Ms* of the compressor for four kinds of nonaxisymmetrical SRCTs at different speeds. Obvious differences among the SCRTs can be noticed from this figure. Together with the static pressure distribution near the leading edge of the splitter blades, as shown in Fig. 11, the implicit relation between *Ms* and static pressure can be inferred.

When the compressor is operated at 85%*N*, there are two periodic waves in the static pressure distribution. Especially, the minimum values are at approximately 90 deg and 270 deg, while the maximum values are close to 180 deg and 360 deg. On the other hand, the largest S_r of types E and G is located at 90 deg and 270 deg, which is coincident with the minimum value of the static pressure at 85%*N*. For types F and D the circumferential phase of the largest S_r is in accordance with that of the maximum static pressure. Then, in Fig. 12 it can be seen that compressors with types G and E SRCT exhibit the largest *Ms*, while compressors with type F and type D have a smaller *Ms* at 85%*N*. When the compressor is operated at 100%*N* and 105%*N*, the static pressure reaches its minimum value between 180 deg and 270 deg. The largest S_r for type G and type F is located at 180 deg and 270 deg,

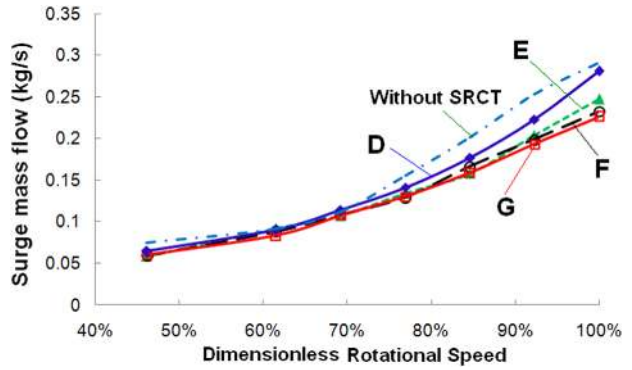

Fig. 10 Comparison of surge flow rates for compressors with nonaxisymmetrical SRCTs

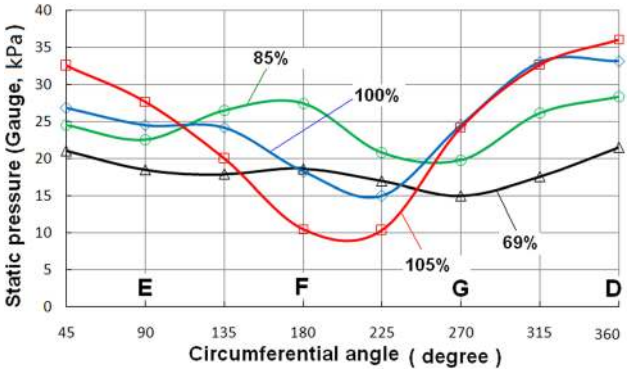

Fig. 11 Static pressure distribution at the leading edge of the splitter blades near surge

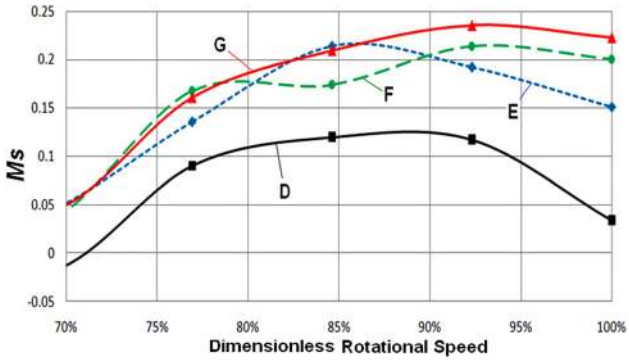

Fig. 12 *Ms* comparison for compressors with different nonaxisymmetrical SRCTs at different rotational speeds

respectively. At these speeds, compressors with types G and F have a larger *Ms* than the compressors with types E and D. It can be concluded from the analysis on these three rotational speeds that the largest *Ms* can be obtained when the phase of the largest S_r of the nonaxisymmetrical SRCT is coincident with that of the minimum value of static pressure near the leading edges of the splitter blades. The stability of the compressor might be deteriorated when the largest S_r is located at the same phase with peak static pressure. Similar results can be drawn from the analysis of other speeds.

5.1.4 Comparison Between Symmetric SRCTs and Nonaxisymmetrical SRCTs. Generally, type C is the best one among the investigated symmetric SRCTs and type G is the best one among the investigated nonaxisymmetrical SRCTs. Figure 13 shows the comparison of surge flow rates of the compressors with types C and G. It is obviously shown in the figure that the surge flow rate of the compressor with type G SRCT is lower than the one with type C. The potential for stability improvement by the nonaxisymmetrical SRCT is larger than by the traditional symmetric SRCT over almost the whole speed range. The average surge flow rate for type G is reduced by 10%, compared with that of type C.

5.2 Simulation Results. Numerical simulation was employed to investigate the influence of different SRCTs on the flow field in the impeller. Figure 14 shows the flow rate in the impeller passages at 100%*N* near surge. The flow rate in each passage is normalized by the design flow rate. Types G and B SRCT were computed and analyzed. It can be seen from Fig. 14 that the SRCT can reduce the flow distortion in the circumferential direction. For compressors with types G and B SRCT, the difference of passage flow rate is smaller than that of the original compressor without SRCT. Furthermore, the flow difference for the nonaxisymmetrical SRCT G is smaller than for the symmetric SRCT B.

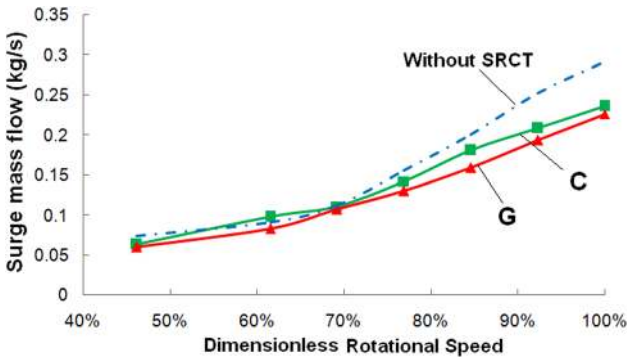

Fig. 13 Comparison of surge flow rate for compressors with type G SRCT and type C SRCT

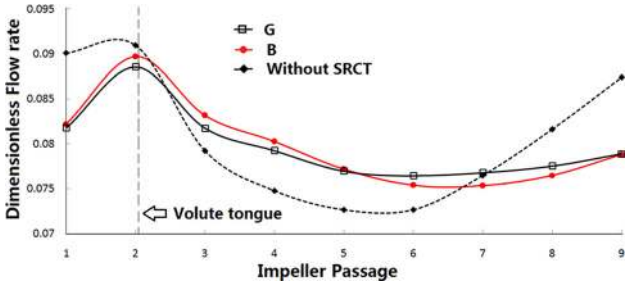

Fig. 14 Flow rate distribution in the impeller passages near surge at 100%*N*

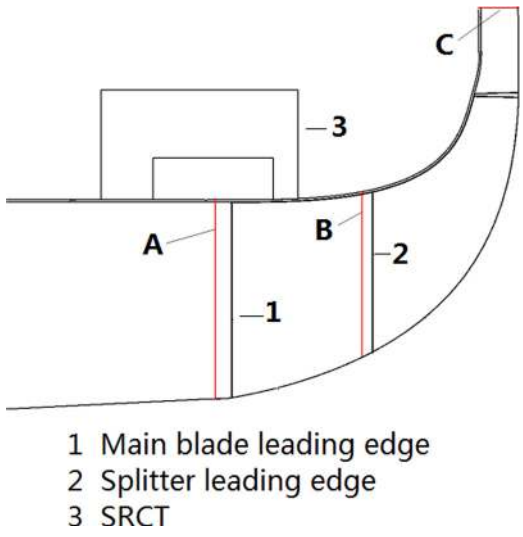

Fig. 15 Sections in compressors with SRCT

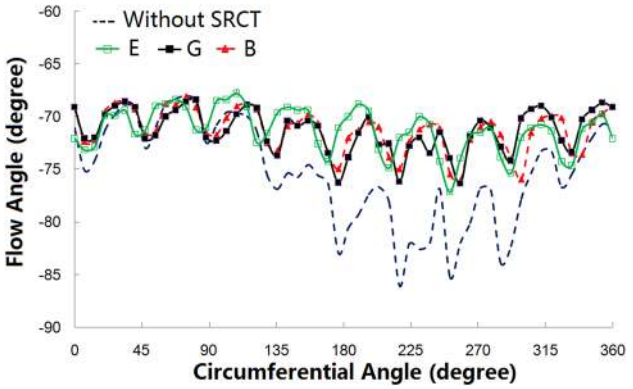

Fig. 16 Relative flow angle distribution near main blade leading edge

According to the analysis presented in part I, the impeller stall initially happens in the passage with the smaller flow rate. Because of the diminished distortion, the impeller stall can be suppressed by the nonaxisymmetrical SRCT.

Figure 15 shows that the compressor has been divided into three sections for analysis. Figures 16–18 show the flow angle distribution at different sections. Figure 16 shows the flow angle near the main blade inlet for different types of casing treatment. For the compressor without SRCT, the flow angle at the inlet is distorted between 135 deg and 315 deg. The incidence decreases sharply and stall is likely to start first in these passages. However, the flow angle becomes much more uniform in the circumferential direction when an SRCT is employed, as shown in Fig. 16 as well. It

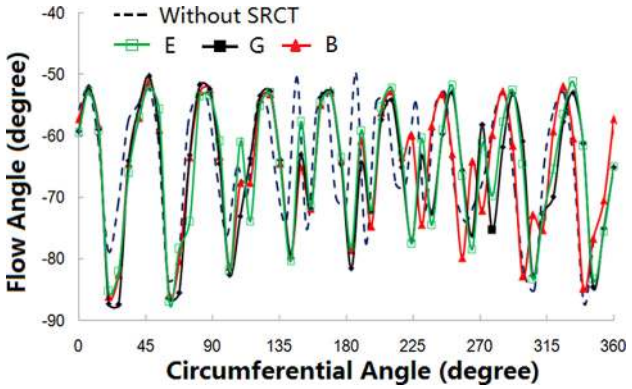

Fig. 17 Relative flow angle distribution near splitter leading edge

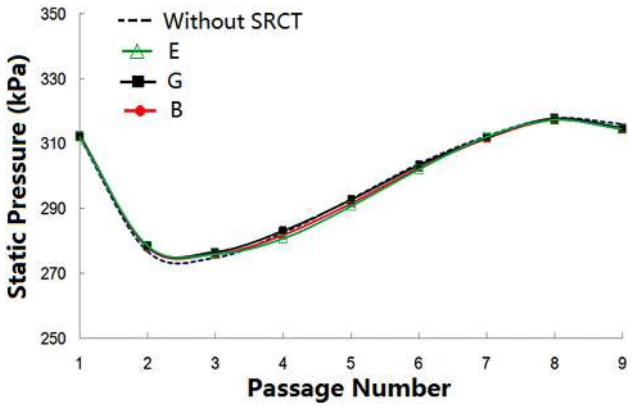

Fig. 18 Static pressure distribution near the outlet of diffuser

can be inferred that this improvement by the SRCT will benefit the stability of the compressor a lot. It is interesting that the angle distribution varies, dependent on SRCT types. Type E with the maximum S_r at 90 deg shows the largest flow angle at around 90 deg–180 deg in the circumferential direction, while type G with maximum S_r at 270 deg shows the largest flow angle around 270 deg–360 deg. Type B with the same S_r in the circumferential direction shows moderate flow angles at all positions. It can be inferred that larger S_r can improve the flow angle at the main blade inlet, which will benefit the flow stability of the impeller.

Figure 17 shows the relative flow angle upstream of the leading edge of the splitter blades. It is quite different from the situation at the inlet discussed above. The flow angle at this section is similar for the different configurations with or without SRCT. The flow angle distortion in the impeller at this section is not as evident as that at the main blade inlet. It implies that the SRCT has little impact on the flow in the rear part of the impeller passages.

Figure 18 shows the circumferential static pressure distribution near the outlet of the diffuser. An evidential flow distortion is present in passages 2 and 3 for all configurations. Besides, the discrepancy of pressure is so small that it can even be neglected. It can be inferred that the SRCT has little influence on the flow in the diffuser. It is also inferred from Figs. 16–18 that the improvement of stability via nonaxisymmetric SRCT is derived by reforming the flow field in the impeller.

The recirculation flow rate distributions via SRCT are shown in Fig. 19. The flow rate is dimensionless by the designed flow rate. It can be noticed that the distributions are evidently different among different kinds of SRCT. The maximum recirculation flow rate locates around 135 deg for type E, 280 deg for type G. The locations could be considered to be in accordance with locations of the maximum S_r for different types of asymmetrical SRCT, although some discrepancies exist between the two locations. The

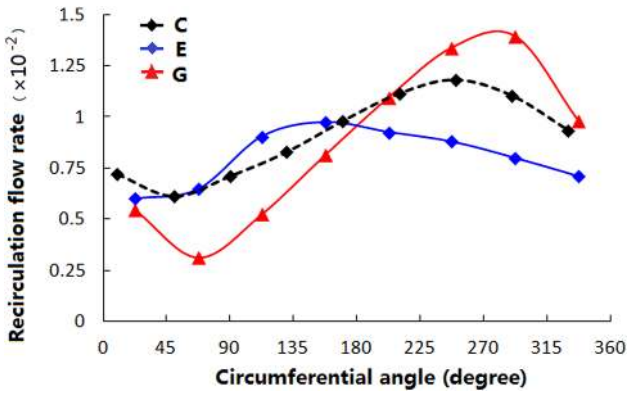

Fig. 19 Relative flow angle distribution near main blade leading edge

maximum recirculation flow rate exits around 240 deg for type C. The recirculation flow rate is not uniform in the circumferential direction even for axisymmetrical SRCT. The nonuniform distributed recirculation flow rate at the impeller inlet depresses the inlet flow distortion in a different way for different SRCT.

When the centrifugal compressor is operated near surge condition, the SRCT sucks in the low momentum flow into the casing and forces it to recycle to the front slot which is located at the shroud near the impeller inlet. Therefore, the incidence is reduced and the surge margin is improved. The larger the inverse pressure gradient in the SRCT, the more the flow will recycle. However, because of the nonaxisymmetrical volute and its interaction with the impeller, obvious asymmetries in the circumferential direction can be found throughout the compressor, which was shown in part I. The pressure gradient between the two slots is not annulus uniform even for a symmetrical SRCT, thus the recirculation flow rate distribution is not axisymmetrical. Furthermore, the magnitude as well as the phase of the distortion varies with the rotational speed. In order to obtain enough inverse pressure gradient, S_r should be larger at the phase where the static pressure is lower. It is indicated that when the distribution of S_r in the circumferential direction is coincident with that of the static pressure near the leading edge of the splitter blades, the pressure gradient in the SRCT can be more uniform in the circumferential direction and the effect of surge margin improvement can be optimized.

6 Conclusions and Remarks

Based on the flow analysis presented in part I, this part documents the development of the nonaxisymmetrical SRCT and investigations of its impact on the flow range of a centrifugal compressor by experiment and numerical simulation. Several conclusions can be drawn as follows:

1. Among the geometric parameters of a symmetric SRCT, the distance between the main blade leading edge and the rear groove of the SRCT and its width have the greatest impact on the performance of a centrifugal compressor.
2. An optimized asymmetrical SRCT is more effective in the compressor stability enhancement than by a symmetrical one. For the SRCT investigated in this paper, the average surge flow rate of the compressor with nonaxisymmetrical SRCT (type G) is about 10% lower than that of the compressor with symmetric SRCT (type C).
3. The largest surge margin (smallest surge flow rate) can be obtained when the phase of the largest S_r is coincident with the phase of the minimum static pressure in the vicinity of the leading edge of the splitter blades.
4. The nonaxisymmetrical SRCT can reduce the circumferential flow distortion at the inlet of the main blades. The nonaxisymmetrical SRCT has little impact on the flow field in the diffuser.

Acknowledgment

This research was supported by the National Natural Science Foundation of China (Grant No. 51176087).

Nomenclature

b_b = width of the horizontal groove of SRCT
b_f = width of front groove of SRCT
b_r = width of rear groove of SRCT
CT = casing treatment
h_b = height of groove of SRCT
FNMB = full nonmatching boundary condition
M = flow rate
Ms = dimensionless surge margin
N = designed rotational speed
P = static pressure
P_t = total pressure
p_r = total to total pressure ratio
R/S = rotor/stator
rev/min = revolutions per minute
S_f = distance between main blade leading edge and front groove of SRCT
S_r = distance between main blade leading edge and rear groove of SRCT
SRCT = self-recirculation casing treatment

Subscripts

org = compressor without SRCT

References

[1] Zhu, D. X., 1992, "Turbocharging and Turbocharger," China Machine Press (in Chinese).
[2] Clenci, A. C., Descombes, G., Podevin, P., and Hara, V., 2007, "Some Aspects Concerning the Combination of Downsizing With Turbocharging, Variable Compression Ratio, and Variable Intake Valve Lift," Proc. Inst. Mech. Eng. Part D, **221**(10), pp. 1287–1294.
[3] Maiboom, A., Tauzia, X., and Héteta, J. F., 2008, "Experimental Study of Various Effects of Exhaust Gas Recirculation (EGR) on Combustion and Emissions of an Automotive Direct Injection Diesel Engine," Energy, **33**(1), pp. 22–34.
[4] Plohberger, D. C., Fessl, T., Gruber, F., and Herdin, G. R., 1995, "Advanced Gas Engine Cogeneration Technology for Special Applications," ASME J. Eng. Gas Turbines Power, **117**(4), pp. 826–831.
[5] Krain, H., Karpinski, G., and Beversdorff, M., 2001, "Flow Analysis in a Transonic Centrifugal Compressor Rotor Using 3-Component Laser Velocimetry," ASME paper No. 2001-GT-0315.
[6] Guo, G. D., Zhang, Y. J., Zheng, X. Q., Xu, J. Z., and Zhuge, W. L., 2008, "Vortex Flows in the Blade Tip Region of a Transonic Centrifugal Compressor," J. Tsinghua Univ. (Sci. Technol.), **48**(11), pp. 1980–1984 (in Chinese).
[7] Arnulfi, G. L., Blanchini, F., Giannattasio, P., Micheli, D., and Pinamonti, P., 2006, "Extensive Study on the Control of Centrifugal Compressor Surge," J. Power Energy, **220**(3), pp. 289–304.
[8] Arnulfi, G. L., Giannattasio, P., Giusto, C., Massardo, A. F., Micheli, D., and Pinamonti, P., 1999, "Multistage Centrifugal Compressor Surge Analysis: Part II—Numerical Simulation and Dynamic Control Parameters Evaluation," ASME J. Turbomach., **121**(2), pp. 312–320.
[9] Saha, S. L., Kurokawa, J., Matsui, J., and Imamura, H., 2001, "Passive Control of Rotating Stall in a Parallel-Wall Vaned Diffuser by J-Grooves," ASME J. Fluids Eng., **123**(3), pp. 507–515.
[10] Asaga, Y., Mizuki, S., Tsujita, H., and Ohta, S., 2008, "Surge Control of a Centrifugal Compression System by Using a Bouncing Ball," J. Thermal Sci., **17**(2), pp. 141–146.
[11] Fisher, F. B., 1989, "Application of Map Width Enhancement Devices to Turbocharger Compressor Stages," SAE Trans., **97**(6), pp. 1303–1310.
[12] Ishida, M., Sakaguchi, D., and Ueki, H., 2005, "Optimization of Inlet Ring Groove Arrangement for Suppression of Unstable Flow in a Centrifugal Impeller," ASME Paper No. GT2005-68675.
[13] Xiao, J., Xu, W., Gu, C. G., and Shu, X. W., 2009, "Self-Recirculating Casing Treatment for a Radial Compressor," Chin. J. Mech. Eng., **22**(4), pp. 567–573 (In Chinese).
[14] Hu, L. J., Yang, C., Qi, M. X., and Ma, C. C., 2009, "Numerical Investigation and Comparison on the Stall Improvement Mechanism of Centrifugal Compressor With Inducer Casing and Bleeding," Chin. J. Mech. Eng., **45**(7), pp. 138–144 (in Chinese).
[15] Hunziker, R., Dickmann, H. P., and Emmrich, R., 2001, "Numerical and Experimental Investigation of a Centrifugal Compressor With an Inducer Casing Bleed System," J. Power Energy, **215**(6), pp. 783–791.
[16] Liu, J. Y., Yuan, W., and Lu, Y. J., 2009, "Experimental Investigation About the Circumferential Treating Angle of Non-axisymmetric Casing Treatments," J. Aerosp. Power, **24**(6), pp. 1385–1388. Available at: CNKI:SUN:HKDI.0.2009-06-030 (In Chinese)
[17] Park, K. Y., 1998, "Non-uniform Compressor Flow Fields Induced by Non-Axisymetric Tip Clearance," Ph.D. thesis, Inha University, Korea.
[18] Graf, M. B., Wong, T. S., Greitzer, E. M., Marble, F. E., Tan, C. S., Shin, H. W., and Wisler, D. C., 1998, "Effects of Nonaxisymmetric Tip Clearance on Axial Compressor Performance and Stability," ASME J. Turbomach., **120**(4), pp. 648–661.
[19] Menson, S., Furman, A., and Krok, M., 2006, "Detection of Surge Precursors in Locomotive Turbocharger," IEEE International Conference on Information Technology, pp. 3067–3071.
[20] Mizuki, S., Asaga, Y., Ono, Y., and Tsujita, H., 2006, "Investigation of Surge Behavior in a Micro Centrifugal Compressor," J. Thermal Sci., **15**(2), pp. 97–102.
[21] Jungowski, W. M., Weiss, M. H., and Price, G. R., 1996, "Pressure Oscillations Occurring in a Centrifugal Compressor System With and Without Passive and Active Surge Control," ASME J. Turbomach., **118**(1), pp. 29–40.